23rd ABCM International Congress of Mechanical Engineering
December 6-11, 2015, Rio de Janeiro, RJ, Brazil

MODELING OF MACRO-EMULSION FLOODING WITH CAPILLARY-DRIVEN EFFECTS

Ranena V. Ponce Flores
Márcio S. Carvalho
PUC-Rio, Department of Mechanical Engineering, R. Marquês de São Vicente 225, Gávea, 22453-900, Rio de Janeiro, RJ - Brazil
poncerv@puc-rio.br, msc@puc-rio.br

Vladimir Alvarado
University of Wyoming, Department of Chemical and Petroleum Engineering, Laramie, WY 82071, U.S.A.
valvarad@uwyo.edu

Abstract. *Capillary forces play a significant role during multiphase fluid flow in porous media as multiphase fluid interfaces control fluid distribution equilibria at the myriad of interconnected or isolated menisci. Capillary number is a key parameter in emulsion designs for EOR purposes. Pore-scale displacement of an emulsion dispersed phase results from the competition of viscous forces, which drives the drops transport through the pores, and capillary forces, responsible for drops entrapment in pore throats. In this work we incorporate capillary-driven effects in two known mechanism observed in water-alternated-emulsion (WAE) injection, namely a microscopic increased pore-level efficiency and a macroscopic mobility control. To properly parametrize relative permeability curves as functions of the capillary number along with the emulsion dispersed phase concentration, a Matlab open source code was modified. A parametric analysis of a ¼ five-spot geometry used on the first layer of the Tabert formation shows that capillary number significantly impacts mobility control potential of the emulsion shown to be responsible for the extra oil recovery. Emulsions with suited drop-to-pore size distribution and interfacial properties optimize emulsion mobility control and sweep efficiency, since heterogeneities in capillary pressure impact emulsion performance and not only flow rate. Results show that mitigation of high injection pressure is possible during cyclic WAE injection without oil recovery impairment.*

Keywords: *Emulsions, Capillary number, Mobility control, Enhanced oil recovery, Two-phase flow.*

1. INTRODUCTION

Fundamental studies in emulsion single-phase flow have shown a reduction of water mobility after emulsion injection (McAuliffe, 1973b, Hofman, et al., 1991). This effect can be interpreted as a water relative permeability reduction during macro-emulsion flooding, which in turn improves water injection profiles (McAuliffe, 1973a). This effect is possible during water-alternated emulsion (WAE) injection, because emulsions can served as mobility control agents based on capillary resistance (Jamin, 1861). Under this mechanism, drops retained in the pore bodies are released only when the local pressure drop is high enough to deform the drops and force them through pore throats.

Cobos, et al., 2009 measured the pressure-drop-flow rate response in constricted micro-capillaries during the flow of emulsions with different drop sizes and dispersed phase viscosity as well as with the continuous phase (without drops). The emulsion continuous phase pressure drop ratio (namely, mobility reduction factor) was analyzed as function of the local capillary number. It was observed that for emulsions with drops size similar to throat radius or larger, the higher the capillary number the lower the pressure drop response, making the mobility reduction factor approach unity. A similar effect was observed at low capillary number, where the threshold pressure to deform the droplet interface is larger than the viscous pressure drop, so the mobility reduction factor becomes much smaller than one. However, between the low and high critical capillary number bounds, a transition zone exists in which the mobility reduction factor is a strong function of the local velocity.

Guillen, et al., 2012 studied the capillary number dependence of emulsion mobility in sandstones and their impact on oil recovery during WAE processes. The authors found that below a characteristic critical capillary number, the mobility reduction factor fell abruptly, so emulsion drops remained trapped while at high capillary number there was almost no effect. Experimental WAE flooding experiments in two similar cores showed that at capillary numbers below the critical value, 20% extra oil recovery was attained after two alternated emulsion slugs. A higher inlet pressure plateau evidenced that the additional oil came from unswept areas resulting from mobility control induced by the blockage of the preferential paths. This effect was ineffective at high capillary number, where only 5% extra oil was recovered after three cycles of water-alternated emulsion injection.

During WAE injection capillary driven effects rule fluid transport or entrapment in the pores being responsible for the extra oil recovery attained after waterflooding. The first effect is enhanced pore -level displacement efficiency caused by the trapping of emulsion oil drops, flow diversion and consequent mobilization of residual oil. The second effect is improved macroscopic (volumetric) sweep efficiency by decreasing water mobility, which stabilizes the injection front and reduces the formation of viscous fingering.

Different approaches have been used to model capillary driven effects on partial plugging of pores by emulsions. Soo and Radke, 1984 studied velocity effects on drops transport during straining and interception regimes in sandpacks. Theoretical analyses for diluted stable O/W emulsions correlates experimental range of critical capillary number where capture, breakup or percolation of the drops occurs. Although the authors had a good agreement between theoretical and experimental permeability reductions, the model did not take into account the variation of the straining and capturing rates with the local capillary number.

More recently, Romero, et al., 2011 developed a capillary network model that uses experimental pore-level flow information from a single constriction in a large capillary network of connected pores. The model predicts microscopic capillary effects from the solution of the local flow equations within each pore. A qualitatively match of capillary number dependence on the mobility reduction factor was found between numerical and experimental results during single flow of emulsions in sandstones. However the model assumed steady state and constant dispersed-phase concentration throughout the network. Nogueira, et al., 2013 improved the latter model by allowing transients and drop concentration gradients to occur, hence enabling residual drop trapping after waterflooding and the consequent flow pattern change.

In our previous work (Ponce, et al., 2014) the flow of diluted stable o/w emulsions was modeled through increased pore-level displacement efficiency (DE) and macroscopic mobility control (MC). Both mechanisms were implemented in a commercial simulator (CMG-STARS) through modifications of the relative permeability curves, so that features of the emulsion (drop-size distribution) as well as their interaction with the rock and the oil (pore size distribution/geometry, interfacial tension, viscosity ratio, etc.) were embedded. In the first mechanism, the relative permeability end-point saturation was parametrized with respect to the dispersed phase concentration to allow microscopic mobilization of the residual oil after waterflooding, while in the second mechanism, macroscopic mobility control was modeled through the reduction of the relative permeability end-point of the water phase.

Since displacement of the emulsion dispersed phase at pore scale is dominated by the competition of viscous and capillary forces, addition of capillary effects is needed. In this paper, we improved our previous model by incorporating capillary effects through an additional parametrization of the relative permeability curves.

2. EMULSION SIMULATION MODEL

Based on the experimental observations of Cobos, et al., 2009 and Guillen, et al., 2012 we improved our previous model by adding necessary capillary effects. In this work, we developed a pseudo-compositional two-phase flow model to parametrize the relative permeability curves as function of emulsion concentration and local capillary number.
All the assumptions of the previous model were kept, i.e. we model the flow of a constant drop size, stable, dilute o/w emulsion. Additionally, the dispersed phase fraction is lower than 10%. At these concentrations, emulsions behave as Newtonian fluids with viscosity similar to that of water. The dispersed phase of the emulsion is considered a component in water, so that the water phase relative permeability curve represents the emulsion relative permeability curve with zero emulsion concentration. There is only one oleic phase saturating the porous media and one water-oil relative permeability set not dependent on capillary number. To incorporate capillary number effects into the previous model we assumed, for simplicity, a linear dependence of the Corey's model (Corey, 1954) parameters as functions of the capillary number *Ca*, defined as $Ca = \mu v/\sigma$, where μ is the viscosity of the displacing fluid, v is the Darcy velocity and σ is the two-phase interfacial tension.

According to experimental observations, we defined two critical capillary numbers (Ca_{min} and Ca_{max}) that establish the block-percolation mechanism of emulsion flooding. The interpolation is made first on capillary number and then on the emulsion dispersed phase concentration as follows. Consider an emulsion with dispersed drop concentration Ce for capillary numbers below Ca_{min}. Under these conditions, the kr-curve corresponds to the pure emulsion set. In contrast, for capillary numbers higher than Ca_{max}, relative permeability corresponds to waterflooding. For capillary numbers between Ca_{min} and Ca_{max}, the emulsion kr-curves results from the linear interpolation between Corey's model parameters for pure emulsion and water phase, namely residual oil saturation to emulsion (Sore*), emulsion relative permeability endpoint at residual oil (Kreor*), and water and oil Corey's exponents respectively (nw*, no*). For the sake of simplicity we assume that the oil relative permeability endpoint for the oil-water and oil-emulsion system were the same (Krowi=Krei=1). A sketch of the interpolation model used to address capillary effects is shown in Fig. 1. Once capillary number dependency is addressed for the pure emulsion, drop concentration effects are accounted for by recalculating new Corey's parameters now for the emulsion as a water phase component. Keeping the same description of the previous model we defined two critical drop concentrations (Ce_{min} and Ce_{max}) to calculate new values for Sore**, Kreor**, nw** and no** through linear interpolations between the water phase and the calculated emulsion kr-curves parameters parametrized by capillary number.

To properly implement the two-phase emulsion flooding model as function of capillary number and dispersed phase concentration in a numerical reservoir simulator we used the open-source code MRST – Matlab Reservoir Simulation Toolbox developed by Aarnes, et al., 2007. We modified the original code from the simplified Black-oil model to add the emulsion transport equation along with the corresponding boundary and initial conditions.

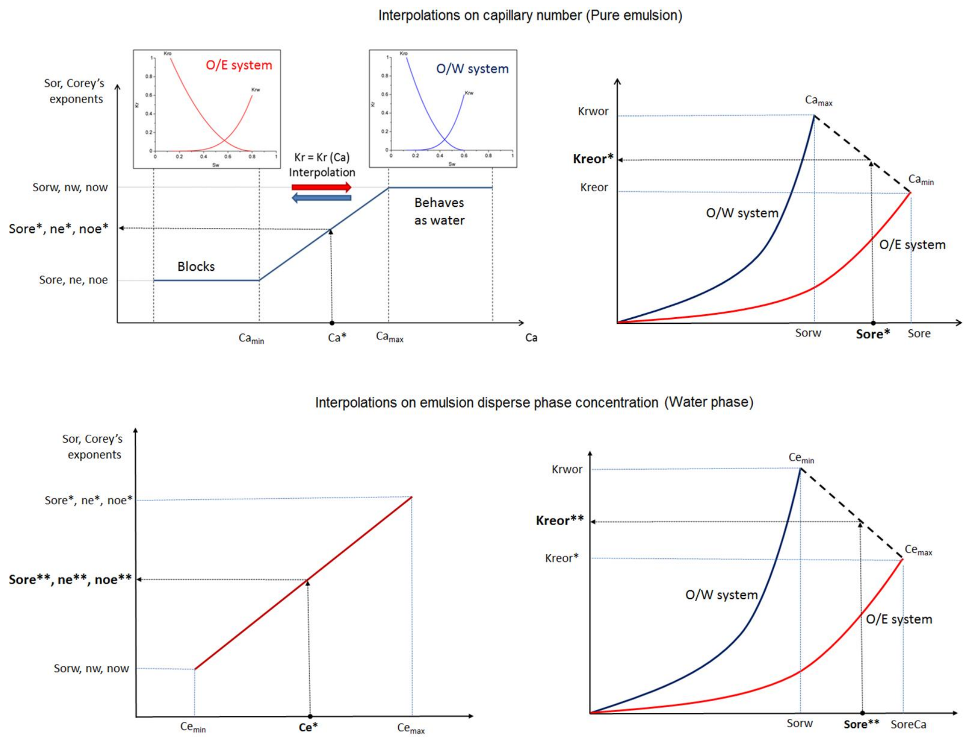

Figure 1. Interpolation model used to account capillary number effects in previous model (Ponce, et al., 2014).

In our description, we assume purely convective transport of the drops, isothermal flow, incompressible fluids and two-phase flow displacement (oil and water). The resulting discretized system of equations are solved by the finite-volume method and partially decoupled in time step by using the implicit pressure, explicit saturation method (IMPES). In the proposed model, it is important to note that since each cell has a local value of drop concentration and capillary number, relative permeability curves of the oil-emulsion system change along the discretized domain such that they are no longer a single function of the water saturation.

3. RESULTS AND DISCUSIONS

To evaluate the model in a highly heterogeneous reservoir, we simulate WAE injection on the first layer of the 10^{th} SPE Comparative Solution Project. The model consisted of 365.76 x 670.56 x 0.61 m^3 described using 60 x 220 x 1 cells. Figure 2 shows absolute permeability and porosity fields (near shore environment- Tabert formation) of this model.

We considered an injector and producer well arranged in an ¼ five spot configuration. Waterflooding and WAE injection was modeled for light oil with oil-water viscosity ratio of $\mu_o/\mu_w = 10$ and oil-water interfacial tension of σ=0.024 N/m. The emulsion concentration at the injector well was $Ce = 1$ and the same value of $\mu_w = \mu_e = 0.001$ Pa.s for water and emulsion viscosity. The oil-water and oil-emulsion set of relative permeabilities for light-oil in a weakly water-wet porous media were described by the Corey model. The emulsion displacement efficiency effect was modeled through the reduction of the residual oil saturation of the water phase, whereas for the mobility control effect the oil residual saturation and the water relative permeability endpoint were reduced. It is important to note that in the displacement efficiency effect, reduction of the water mobility results naturally by reduction of the oil residual saturation, so the name of each mechanism was selected in order to highlight the more pronounced effect in each one of them. Figure 3 shows the set of kr-curves used in the simulations.

The constraints in the simulations were set at $Q = 1.082 \times 10^{-4}\ m^3/s$ for injector and atmospheric bottom-hole pressure for the producer. Two critical capillary numbers used for kr-curves interpolations were calculated numerically to account for flow features associated to the geological model. As capillary number distribution in the injection geometry falls radially from the injection point, we selected the lower capillary number so that fluid mobility near the injector well remains high enough for the emulsion to reach deeper locations in the reservoir where mobility control is needed. To this end, the minimum value was obtained at a radial distance equal to the half of the x-length of the reservoir, which results in $Ca_{min} \simeq 5.62 \times 10^{-9}$. For the sake of simplicity we chose the threshold on maximum capillary number as $Ca_{max} = 10Ca_{min}$. For water-alternating emulsion injection we selected waterflooding for 0.1 pore volumes (PV) followed of 1 PV of emulsion chased for water injection to complete a total of 5 PV injected of fluids.

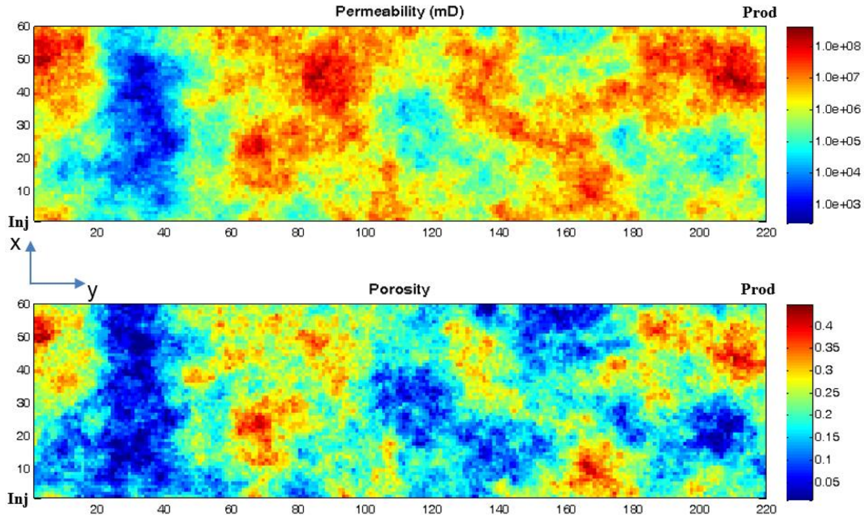

Figure 2. Absolute permeability and porosity fields used in the simulations.

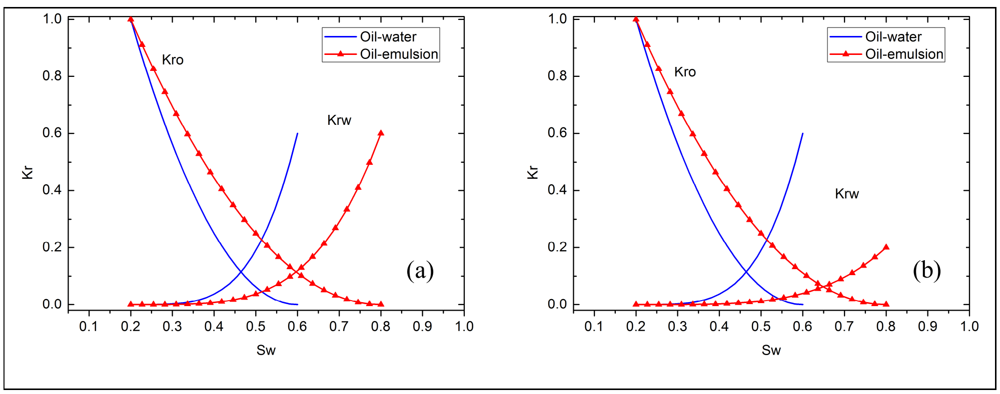

Figure 3. Oil-water and oil-emulsion relative permeability curves used in the simulations to model emulsion capillary-driven mechanisms: (a) Displacement efficiency, (b) Mobility control.

To investigate the effectiveness of the emulsion flow with drop concentration and capillary number dependence we analyzed key parameters that could affect the described capillary-driven mechanisms.

Initially the effect of both mechanisms, mobility control and displacement efficiency, were analyzed by simulating WAE injection at $Q = 1.082 \times 10^{-4}\ m^3/s$. Figure 4 shows the oil recovery factor (RF), water cut (WCUT), Injector bottom-hole pressure (IBHP) and emulsion dispersed phase concentration (*Ce*) as function of the pore volume injected (PV) for waterflooding and WAE injection.

Although there is an approximate 2% difference in RF, the case with pronounced mobility mechanism attained the higher oil recovery (50.19%). Despite the small difference in oil recovery, a high injector bottom-hole pressure for the mobility control mechanism is noted, which could be related to the reduction of the water mobility due to a more intense pore blockage with the consequent diversion of water and mobilization of viscous oil clusters in unswept zones.

One of the undesirable effects of the overall increase in reservoir pressure in practical applications is the potential risk of promoting unwanted fractures and creating early breakthrough. To study the pressure behavior for the mobility control mechanism we model the WAE process, but instead of injecting 1PV of emulsion in a single slug, we injected 10 cycles of 0.1 PV of emulsion. Production results shown in Fig. 5 indicate a reduction of the injector bottom-hole pressure with the WAE injection. The pressure of the displacing fluid is increased in small increments so the overall pressure response is completely dissipated during the cyclic injection of emulsion without significant detrimental in ORF (49.46%).

To investigate the emulsion displacement efficiency response with capillary number we compared the impact of the flow rate against the critical capillary number from which capillary forces become negligible. To this end, we keep constant the flow rate and increased the maximum capillary number 10 times: $Ca_{max} \simeq 5.62 \times 10^{-7}$.

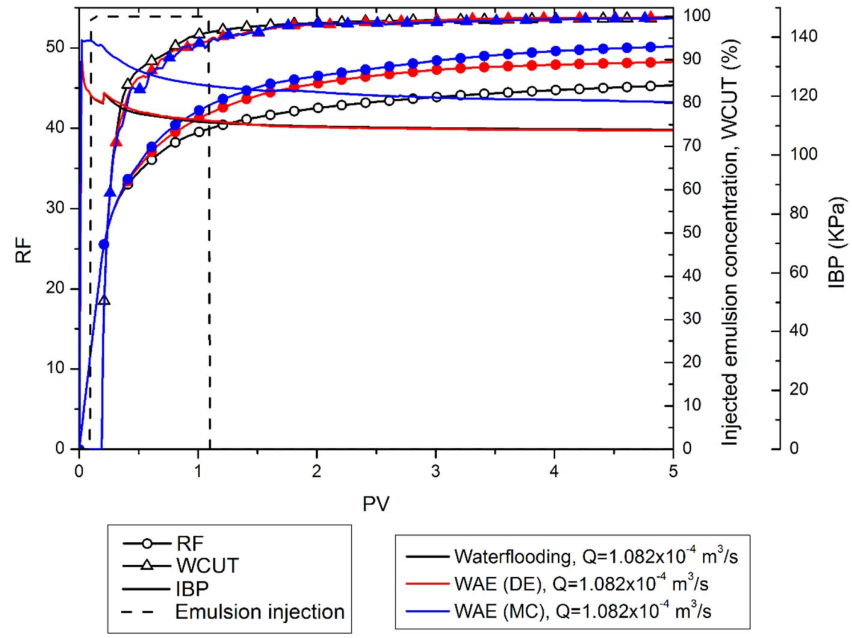

Figure 4. Production results for waterflooding and WAE injection using the mobility control and displacement efficiency mechanisms.

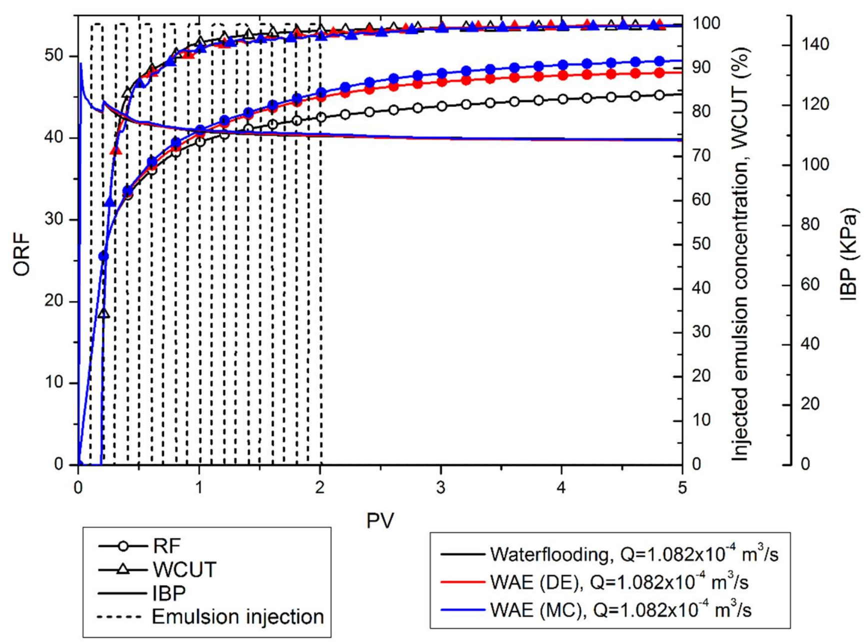

Figure 5. Production results for waterflooding and WAE injection processes using the mobility control and displacement efficiency mechanisms. 1PV of Emulsion was injected in 10 cycles of 0.1 PV.

Figure 6. shows the production results as function of the pore volume injected for waterflooding and WAE injection at $Q = 1.082 \times 10^{-4}\ m^3/s$ for $Ca_{max} \simeq 5.62 \times 10^{-8}$ and $Ca_{max} \simeq 5.62 \times 10^{-7}$ as well as for the lower flow rate case $Q = 1.082 \times 10^{-5}\ m^3/s$ with $Ca_{max} \simeq 5.62 \times 10^{-8}$. Results showed that the highest oil recovery (> 59.31%) is obtained for the low flow rate case $Q = 1.082 \times 10^{-5}$ with $Ca_{max} \simeq 5.62 \times 10^{-8}$ which would be explained by the enhanced water mobility control and a locally better sweep efficiency promoted by strong reduction of the viscous effects. Analyzing the two cases with the same flow rate ($Q = 1.082 \times 10^{-4}\ m^3/s$) it might be noticed a significant difference in oil recovery, i.e. $Ca_{max} \simeq 5.62 \times 10^{-8}$ (48.25%) and $Ca_{max} \simeq 5.62 \times 10^{-7}$ (55.51%). Figure 7 shows emulsion response maps.

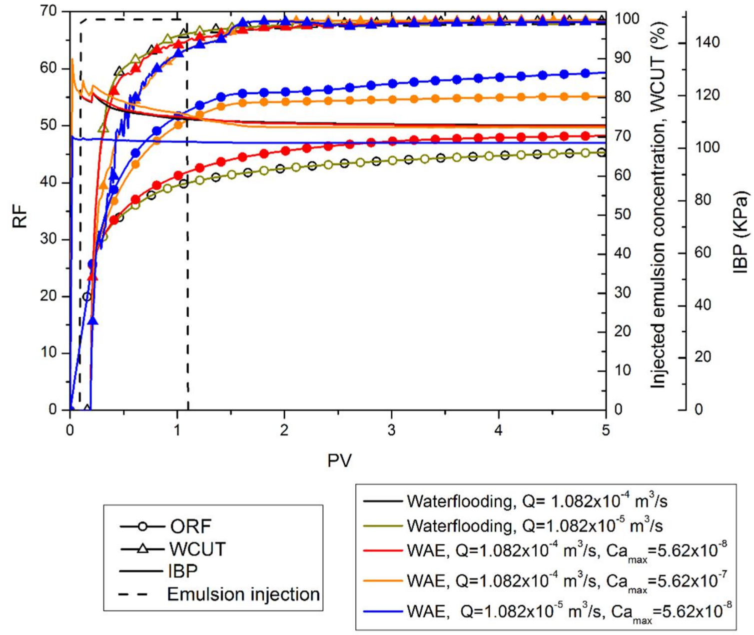

Figure 6. Production results for waterflooding and WAE injection processes to evaluate flow rate effect against maximum critical capillary number (Ca_{max}) - Displacement efficiency mechanism.

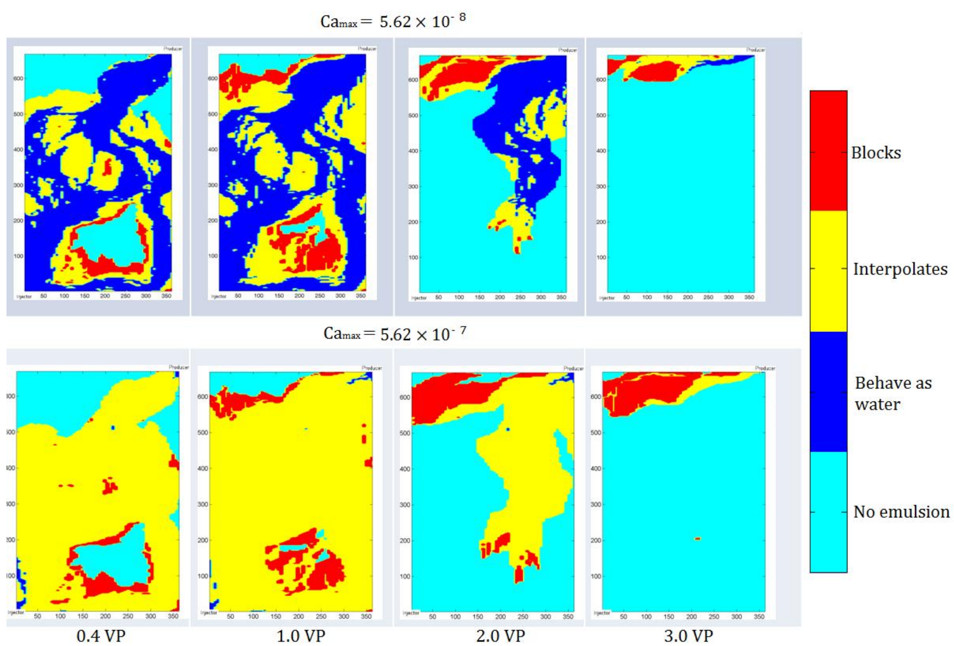

Figure 7. Maps of the behavior of the emulsion as function of the drop concentration and capillary number for WAE injection at $Q = 1.082 \times 10^{-4}\ m^3/s$ for $Ca_{max} \simeq 5.62 \times 10^{-7}$ and $Ca_{max} \simeq 5.62 \times 10^{-8}$ – Displacement efficiency mechanism.

Increasing the threshold at which emulsions will behave as water increases the zone in the reservoir where the competition of viscous and capillary forces takes place. Heterogeneities of the capillary pressure affects locally the dynamics of the fluid interfaces, so increasing the Ca_{max} threshold allow the emulsion to reach larger pores. Since for practical effects the invaded zones are strong functions of the drop-to-pore size distribution (Dd/Dp), results suggest that both, Dd/Dp and flow rate are key parameters to be considered to properly design oil-in-water emulsions.

To investigate the potential of the displacement efficiency mechanism with respect to the mobility control, we simulated WAE injection reducing the flow rate of the DE mechanism to a half of the used in the mobility control case.

Production results are shown in Fig. 8. Comparison between recovery factors obtained for DE mechanism from Fig. 4 (48.25%) and Fig. 8 (50.70%) suggest that reduction of the flow rate promotes a slight acceleration of oil production and increase in the recovery factor. Figure 8 shows that at low flow rate the case with the displacement efficiency mechanism reaches a slightly higher recovery than that associated to mobility control (RF=50.19%).

Maps of the emulsion response for both cases depicted in Fig. 9 suggest that extra oil recovered by the displacement efficiency mechanism at low flow rate is promoted by the increment of zones where the viscous and capillary forces competes for residual oil mobilization/retention. The observed extra recovery can be explained by oil displacement in zones with enhanced microscopic sweep efficiency and capillary forces high enough to suppress water mobility.

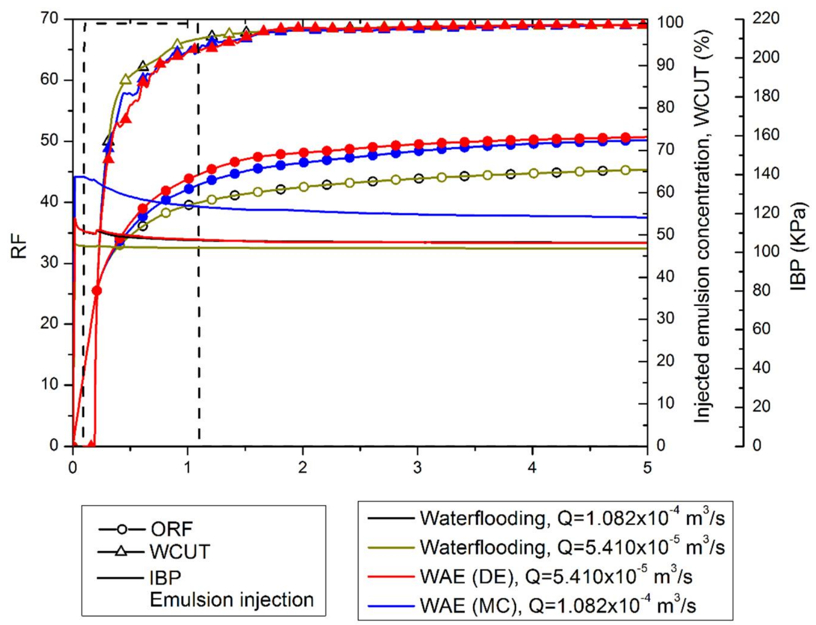

Figure 8. Production results for waterflooding and WAE injection using the mobility control ($Q = 1.082 \times 10^{-4}\ m^3/s$) and displacement efficiency mechanism at half of the flow rate ($Q = 5.41 \times 10^{-5}\ m^3/s$).

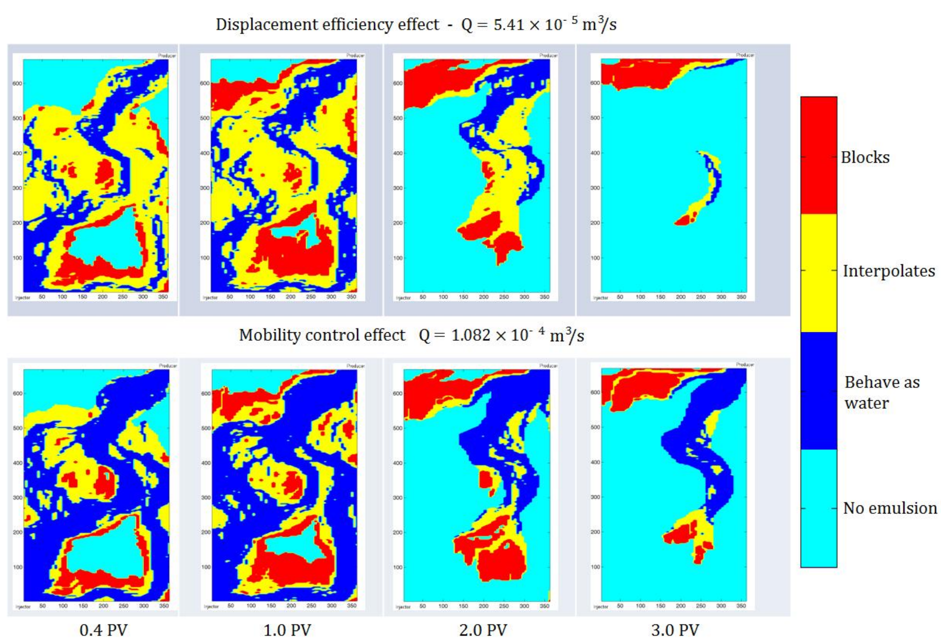

Figure 9. Maps of the behavior of the emulsion as function of the drop concentration and capillary number for mobility control ($Q = 1.082 \times 10^{-4}\ m^3/s$) and displacement efficiency mechanism ($Q = 5.41 \times 10^{-5}\ m^3/s$).

4. CONCLUSIONS

In this paper we modeled capillary driven effects on the displacement of diluted stable oil-in-water emulsions. Two key mechanisms observed experimentally, namely displacement efficiency and mobility control effects were incorporated in an open source code (MRST - SINTEF) by parametrization of the relative permeability curves as function of the concentration of the emulsion dispersed phase and the local capillary number.

Results show that capillary number affects strongly the effectiveness of the emulsion mobility control potential and consequently on ultimate oil recovery. Moreover results showed that flow rate alone does not affect the emulsion performance, but heterogeneities of the capillary pressures along the fluids interfaces as well, so emulsions with designed drop-to-pore size distribution and tailored interfacial properties offer a good potential to improve oil recovery. Water mobility control effect was shown to be responsible for additional oil recovery, promoting diversion of water by blockage of the waterflooded high capillary number reservoir zones. Attenuation of high injection pressure due to pore blockage and water diversion during emulsion injection can be achieved by cyclic injection of smaller slugs without detrimental in oil recovery.

Further work is needed to incorporate into the model related capillary trapping and drop to pore size distribution effects on the emulsion performance.

5. ACKNOWLEDGEMENTS

We would like to acknowledge the Chevron Corporation, Petrobras and the Enhanced Oil Recovery Institute (EORI) at the University of Wyoming for financial support.

6. REFERENCES

Aarnes J.E., Gimse T., Lie K.A, 2007. *An Introduction to the Numerics of Flow in Porous Media using Matlab*, Geometric Modelling, Numerical Simulation, and Optimization Applied Mathematics at SINTEF, 265-306.

Cobos S., Carvalho M., Alvarado V., 2009. *Flow of oil-water emulsions through a constricted capillary*, International. Journal of Multiphase Flow 35, 507–515.

Corey A.T., 1954. *The Interrelation Between Gas and Oil Relative Permeabilities*. Prod. Monthly 19 (1), 38–41.

Guillen V. and Romero M. and Carvalho M. and Alvarado V., 2012. *Capillary-driven mobility control in macro emulsion flow in porous media*, International Journal of Multiphase Flow 43, 62–65.

Hofman, J. A.M.H. and Stein, H. N., 1991, *Permeability reduction of porous media on transport of emulsions through them*. Colloids and Surfaces 61, 317-329.

Jamin, J., 1861. *Leçons sur les lois de l'équilibre et du mouvement des liquides dans les corps poreux*, Paris. In Bickerman, J. J.: *Swjace Chemistry for Industrial Research*, Academic Press Inc., New York (1948) 330.

McAuliffe, C. D., 1973a*, Crude-oil-in-water emulsions to improve fluid flow in an oil reservoir*, SPE Journal of Petroleum Technology 25 (6), 721-726.

McAuliffe, C. D., 1973b, *Oil-in-water emulsions and their flow properties in porous media*, SPE Journal of Petroleum Technology 25 (6), 727-733.

Nogueira G.L and Carvalho M. S and Alvarado V., 2013. *Dynamic Network Model of Mobility Control in Emulsion Flow Through Porous Media*, Transport in Porous Media 98 (2), 427-441.

Ponce F.R.V. and Carvalho M. and Alvarado V., 2014. *Oil recovery modeling of macro-emulsion flooding at low capillary number*. Journal of Petroleum Science and Engineering 119, 112–122.

Romero M.I and Carvalho M. and Alvarado V., 2011. *Experiments and network model of flow of oil-water emulsion in porous media*. Physical Review E 84, 046305.

Soo H. and Radke C., 1984. *Velocity effects in emulsion flow through porous media*, Journal of Colloid and Interface Science 102 (2), 462–476.

7. RESPONSIBILITY NOTICE

The authors are the only responsible for the printed material included in this paper.